ACS chemical biology

Articles

pubs.acs.org/acschemicalbiology

Genome Editing-Enabled HTS Assays Expand Drug Target Pathways for Charcot–Marie–Tooth Disease

James Inglese,*[,†,‡] Patricia Dranchak,[†] John J. Moran,[§] Sung-Wook Jang,[†] Rajini Srinivasan,[§] Yolanda Santiago,[∥] Lei Zhang,[∥] Rajarshi Guha,[†] Natalia Martinez,[†] Ryan MacArthur,[†] Gregory J. Cost,[∥] and John Svaren*[,§]

[†]National Center for Advancing Translational Sciences, National Institutes of Health, Rockville, Maryland 20850, United States
[‡]National Human Genome Research Institute, National Institutes of Health, Bethesda, Maryland 20892, United States
[§]Department of Comparative Biosciences, and Waisman Center, University of Wisconsin, Madison, Wisconsin 53705, United States
[∥]Sangamo BioSciences, Richmond, California 94804, United States

Supporting Information

ABSTRACT: Copy number variation resulting in excess PMP22 protein causes the peripheral neuropathy Charcot–Marie–Tooth disease, type 1A. To broadly interrogate chemically sensitive transcriptional pathways controlling PMP22 protein levels, we used the targeting precision of TALEN-mediated genome editing to embed reporters within the genetic locus harboring the Peripheral Myelin Protein 22 (*Pmp22*) gene. Using a Schwann cell line with constitutively high endogenous levels of Pmp22, we obtained allelic insertion of secreted bioluminescent reporters with sufficient signal to enable a 1536-well assay. Our findings from the quantitative high-throughput screening (qHTS) of several thousand drugs and clinically investigated compounds using this assay design both overlapped and expanded results from a previous assay using a randomly inserted reporter gene controlled by a single regulatory element of the *Pmp22* gene. A key difference was the identification of a kinase-controlled inhibitory pathway of *Pmp22* transcription revealed by the activity of the Protein kinase C (PKC)-modulator bryostatin.

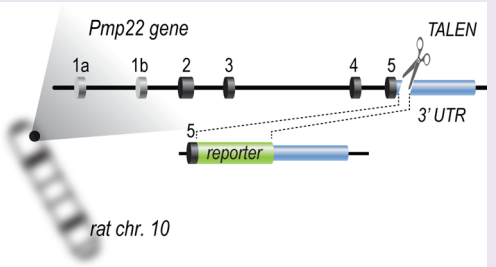

The peripheral neuropathy Charcot–Marie–Tooth disease (CMT) causes progressive deterioration of motor and sensory nerves, muscular atrophy, and chronic pain and fatigue. As one of the most common genetic diseases affecting the nervous system,[1] CMT and more severe neuropathies affect approximately 1 in 3,000 individuals. Current treatment options generally manage symptoms but do not effectively mitigate the underlying causes of these conditions.[2,3] A majority of genetically diagnosed CMT is caused by a 1.5 Mb duplication on chromosome 17 that results in trisomy of the critical myelin gene *Peripheral Myelin Protein 22* (*Pmp22*).[4−7] This duplication is classified as CMT1A. In rodent models, increasing *Pmp22* expression is sufficient to cause a demyelinating phenotype,[8−12] and reducing *Pmp22* expression improves myelination in rodent models of CMT1A.[13−15]

Studies in rodent models of CMT1A have identified two transcription-based strategies that ameliorate the disease by reducing *Pmp22*. High dose ascorbic acid[13] is the basis of a recent clinical trial for therapy of CMT1A. However, the high doses of ascorbic acid required by mice may reflect a lack of potency, and human clinical trials have not shown a significant effect in CMT1A patients.[16] Proof-of-principle studies using progesterone antagonists to reduce *Pmp22* expression in a rat model of CMT have shown beneficial effects,[15] but this molecular class has not advanced to clinical trials. Since these candidate approaches have shown that a relatively subtle (<2-fold) change in *Pmp22* transcription could effectively treat the most common form of inherited peripheral neuropathies, there is a significant need for unbiased approaches toward identification of therapeutic agents for CMT1A.

Our previous studies used chromatin immunoprecipitation analysis (ChIP) to identify functional enhancer elements in the *Pmp22* locus by localizing binding sites for two critical transcription factors that control peripheral nerve myelination, Egr2/Krox20 and Sox10,[17,18] and identified a major regulatory site within one of the introns of the *Pmp22* gene.[19] This enhancer was used to create reporter assays, in which an orthogonal pair of stable Schwann cell lines was engineered with the human version of the *PMP22* regulatory element driving expression of either the firefly luciferase (FLuc) or β-lactamase reporter genes. We performed qHTS of an approved drug library (~3000 compounds),[20] which identified several compounds that inhibit *Pmp22* expression in both reporter assays as well as endogenous *Pmp22*.[21]

A limitation of this assay, however, is that it relies on a single regulatory element of the *Pmp22* gene and does not incorporate possible regulation of the *Pmp22* gene by post-transcriptional mechanisms, including the recently discovered

Received: July 9, 2014
Accepted: September 4, 2014
Published: September 4, 2014

   dx.doi.org/10.1021/cb5005492 | *ACS Chem. Biol.* 2014, 9, 2594–2602

regulation of *Pmp22* expression by microRNAs.[22,23] In addition, the random insertion of the reporter gene may create position effects that prevent the reporters from serving as a faithful proxy for *Pmp22* regulation. Finally, subsequent studies have identified additional regulatory elements for *Pmp22* that reside much further upstream of the gene (>100 kb), which could play a role in *Pmp22* regulation.[24−26] To address these facts and more broadly recapitulate *Pmp22* regulation, we have developed a series of complementary HTS assays by inserting reporters into the endogenous *Pmp22* locus using TALEN-mediated genome editing.[27,28] This enhanced screen validated and extended the spectrum of compounds known to repress *Pmp22* levels. Notably, we identify a protein kinase C (PKC)-dependent regulatory pathway that reduces *Pmp22* levels.

RESULTS AND DISCUSSION

Assay Design and Validation. To explore a broader spectrum of *Pmp22* regulation, we devised a system to assay the effects of small molecules on the expression of *Pmp22* by engineering the gene to express a reporter ORF from the endogenous genomic locus. TALEN technology was used to genetically modify the S16 Schwann cell line,[29] which expresses near physiological levels of *Pmp22* mRNA and has been characterized extensively in ChIP analysis. In general, the binding sites for Egr2 and Sox10 in the *Pmp22* gene in myelinating sciatic nerve are also observed in the S16 cell line,[19,24] indicating that the regulatory environment of *Pmp22* closely mimics the *in vivo* environment.

TALEN pairs were designed to target a sequence near the 3′ end of the *Pmp22* ORF (Figure 1). These TALEN pairs were

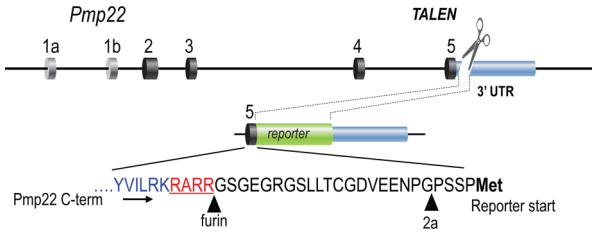

Figure 1. TALEN-based design strategy for genome edited *Pmp22* reporter cell lines. Diagram depicts position of TALEN cleavage within the *Pmp22* gene at the 3′ end of the ORF. After recombination, the native stop codon is fused with a sequence containing a furin cleavage site, followed by self-cleaving 2a sequence and the start codon of the inserted reporter. Triangles indicate positions of cleavage by furin protease and the 2a cleavage site. The indicated reporter is either *Gaussia* luciferase (GLuc) or a nested secNLuc-P2A-GFP sequence that upon expression produces a secreted Nanoluciferase (secNLuc) reporter and GFP that is used for cell sorting and selection.

tested for genome editing activity in S16 cells as gauged by the introduction of small insertions and deletions at the target locus following repair of the nuclease-induced DNA double-strand break (DSB) via non-homologous end-joining. Active TALEN pairs identified in this manner induced a DSB at the stop codon of *Pmp22* (Figure 2A). To insert a reporter ORF into the endogenous *Pmp22* locus, we developed a construct in which two arms of homology flank the TALEN-targeted site at the stop codon of the *Pmp22* gene. As depicted in Figure 1, the TALEN-driven insertion of the reporter at the 3′ end of the *Pmp22* coding sequence permits co-transcription of the reporter as part of the same RNA. PMP22 is fused in-frame with the reporter with an intervening ribosome stuttering signal (viral 2a sequence) that results in release of the PMP22 protein from the ribosome, followed by re-engagement and translation of the reporter ORF.[30] In addition, an introduced furin cleavage site at the junction of PMP22 with 2a results in removal of the 2a sequence. The assay configuration allows comprehensive examination of genetic and epigenetic elements governing *Pmp22* transcription in its native chromatin context.

The reporter chosen for the initial study was *Gaussia* luciferase (GLuc), a secreted protein,[31] which allows non-destructive analysis of clones during expansion to test for successful genome editing. In contrast to luciferases from firefly and *Renilla*, GLuc is a naturally secreted stable protein and thus not susceptible to an intracellular turnover, which permits examination of an alternative mode of inhibition using a loss-of-signal assay. This is important because the assay window ceiling is dependent on the basal *Pmp22* transcription as assessed from monoallelic reporter expression where maximal signal intensities may be relatively low. The recapitulation of *Pmp22* expression by GLuc was validated pharmacologically using the proteasome inhibitor bortezomib (Figure 2B), a drug modulator previously identified.[21] To observe this inhibition, bortezomib was added at the time of plating, since accumulation of reporter activity in the medium would otherwise obscure the effect.

The regulation of the reporter was also tested by using siRNA-mediated depletion of the Sox10 transcription factor known to activate *Pmp22*.[19] Because of the stability of the secreted GLuc, there was no change in secreted reporter activity at 24 h after transfection with siRNA for Sox10 (not shown). However, if the medium was exchanged at 24 h and then reassayed at 48 h, there was a significant reduction in reporter activity in S16 cells in which Sox10 is depleted compared to cells treated with a scrambled siRNA (Figure 2C). Similar results were obtained by exchanging medium 2 h prior to the 48 h time point. In addition to reporter activity, we also examined PMP22 protein levels by Western blot. As shown in Figure 2D, depletion of Sox10 resulted in lowering of PMP22 protein. Although higher molecular weight bands are present at ≥50 kDa, we interpret them to be non-specific since they do not change in response to Sox10 siRNA.

Genome Editing To Insert Tandem Reporters. While the above approach succeeded to create a single cell line expressing GLuc from the endogenous *Pmp22* locus, isolation of additional clones was hampered by low efficiency recombination using this reporter insertion strategy. To develop a more efficient procedure to identify a complementary cell line for screening, we utilized an alternative reporter design in which a secreted nanoluciferase reporter (secNLuc) was co-inserted with a GFP reporter to allow cell sorting of GFP-expressing clones. NLuc is a newly engineered reporter that has a molecular weight substantially lower than that of other luciferases and has high activity with the coelenterazine substrate analogue furimazine[32] yet appears sufficiently distinct from GLuc with regard to interference by confounding inhibitors.[33] In this case, we chose to use the secreted form of NLuc to incorporate the advantages described above for GLuc. In this design, the 2a ribosome stuttering sequence separated all three ORFs, *Pmp22*, GFP, and secNLuc (Figure 1).

After transfection of this reporter, we were able to detect NLuc activity in the supernatant of unsorted cells (not shown). Cell sorting of transfected cells revealed a small number (<0.1%) of GFP positive cells. The cells were sorted a second

dx.doi.org/10.1021/cb5005492 | *ACS Chem. Biol.* 2014, 9, 2594−2602

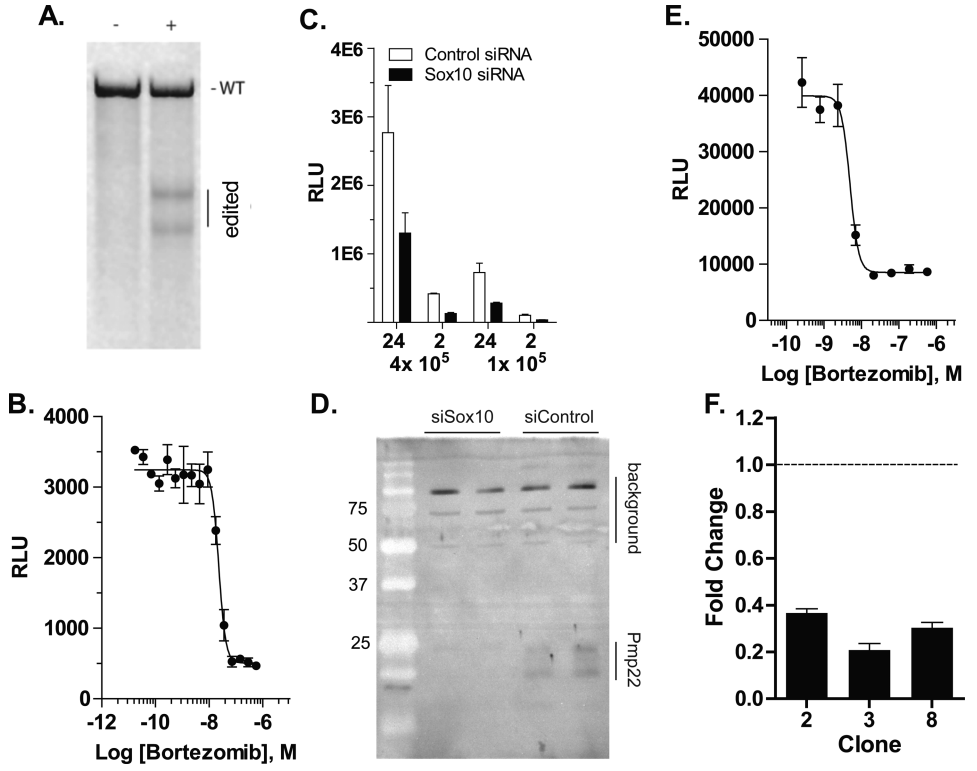

Figure 2. Molecular and pharmacological characterization of *Pmp22* reporter assay using genome editing. (A) Assay of TALEN pairs using a Cel-1 endonuclease assay demonstrates cleavage at the *Pmp22* stop codon with 9.6% efficiency. (B) The S16 Schwann cell line with insertion of *Gaussia* luciferase (GLuc) was exposed to bortezomib at the indicated concentrations, and relative luciferase activity was measured at 24 h after exposure. (C) The S16 reporter line was transfected with either Sox10 siRNA or a scrambled control siRNA, and luciferase activity was measured at 48 h after transfection using two different cell plating concentrations. The medium was replaced at 24 or 2 h prior to measurement as indicated. (D) Lysates from the S16 reporter line were analyzed by immunoblot for PMP22 expression. The doublet of PMP22 is observed in the control siRNA lanes but is absent after transfection with siRNA for Sox10. Background bands at higher molecular weights are indicated. Molecular weight markers (kDa) are shown on the left side. (E) The S16 reporter line with secNLuc was exposed to the indicated concentrations of bortezomib, and NLuc activity was measured at 24 h. (F) Three independent clones of the NLuc assay were transfected with siRNA for Sox10, and activity was measured at 48 h after transfection. The resulting activity is shown relative to the same clones transfected with a control siRNA, which was set as 1.

time (Supplementary Figure 1A), and single cells were distributed into 96-well plates. The secNLuc reporter was used to identify positive clones by measuring enzyme activity in supernatants from individual wells. After expanding positive clones, genomic DNA was obtained from the selected clones and was tested for insertion at the *Pmp22* locus by PCR (Supplementary Figure 1B). Upon plating equal cell numbers of the indicated clones, we obtained remarkably consistent NLuc activities from the 8 positive clones, with a <4-fold range of NLuc activities (Supplementary Figure 1C).

Clones with insertion at the correct locus were further tested using known inhibitors of *Pmp22* expression,[21] giving the response exemplified in Figure 2E for bortezomib treatment. The reporter activity of all tested clones were inhibited by bortezomib, and as shown in Table 1, three independent clones with the incorporated secNLuc reporter exhibited a very similar inhibition pattern with bortezomib, yielding IC_{50}'s between 34 and 39 nM. We also performed a similar test of Sox10-dependency of the secNLuc reporter. As shown in Figure 2F, three independent clones were transfected with siRNA directed against Sox10, and all 3 clones had reduced reporter activity relative to cells transfected with a control siRNA (measured at 48 h after transfection with a media change 2 h prior to measurement). Therefore, the inserted secNLuc reporter exhibits similar drug sensitivity and Sox10 dependence as the native *Pmp22* gene.

Table 1

parameter	clone 2	clone 3	clone 8
average intensity[a] (RLU)	17000	6900	6000
% CV[a]	7.0	7.2	6.3
EC_{50} bortezomib (nM)	34	35	39

[a] n = 768.

Assay Optimization and qHTS Implementation. The S16 gene locus-targeted GLuc and secNLuc assays were scaled to 4 μL volumes in 1536-well plate format as previous described for the randomly integrated *Pmp22* enhancer element-driven FLuc or β-lactamase reporter assays,[21] but with an important protocol modification. Because the reporters used here are secreted into the medium, we added compound within 1 h of delivering cells in fresh medium to the microtiter plates (see protocol Supplementary Table 1). This protocol maintains an acceptable window (4−5-fold) between basal and suppressed reporter transcription over the 24 h incubation period (Supplementary Table 2).

To identify novel inhibitors of *Pmp22* expression, the luciferase reporter lines were used in a qHTS screen of an approved and investigational drug library.[20] In qHTS, library compounds are tested as a titration series to generate concentration−response curves (CRCs) for each compound.

dx.doi.org/10.1021/cb5005492 | ACS Chem. Biol. 2014, 9, 2594−2602

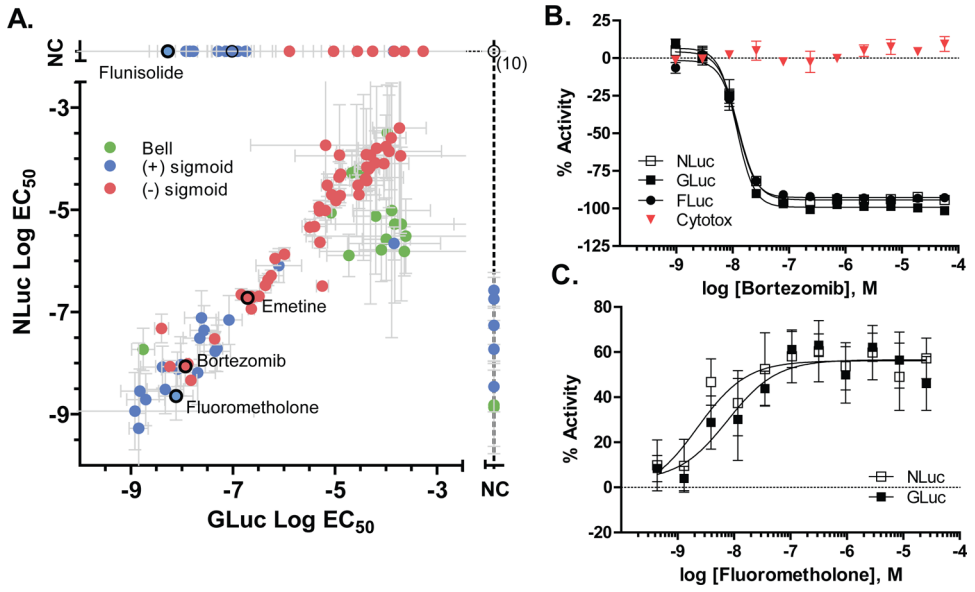

Figure 3. Pharmacologic correlation between S16 GLuc and S16 secNLuc reporter lines. (A) EC_{50} correlation for 121 library compounds and related chemotypes or bioactive classes obtained from reporter lines. For bell curves EC_{50} was derived from ascending portion of the concentration–response curve (CRC). NC indicates error threshold exceeded in one of the assays (see Methods). Data are the mean of $n = 4$, error is the SD. (B, C) Examples CRCs used to derive EC_{50} values for compounds falling on the correlation plot diagonal and showing opposite pharmacological responses, bortezomib and fluorometholone.

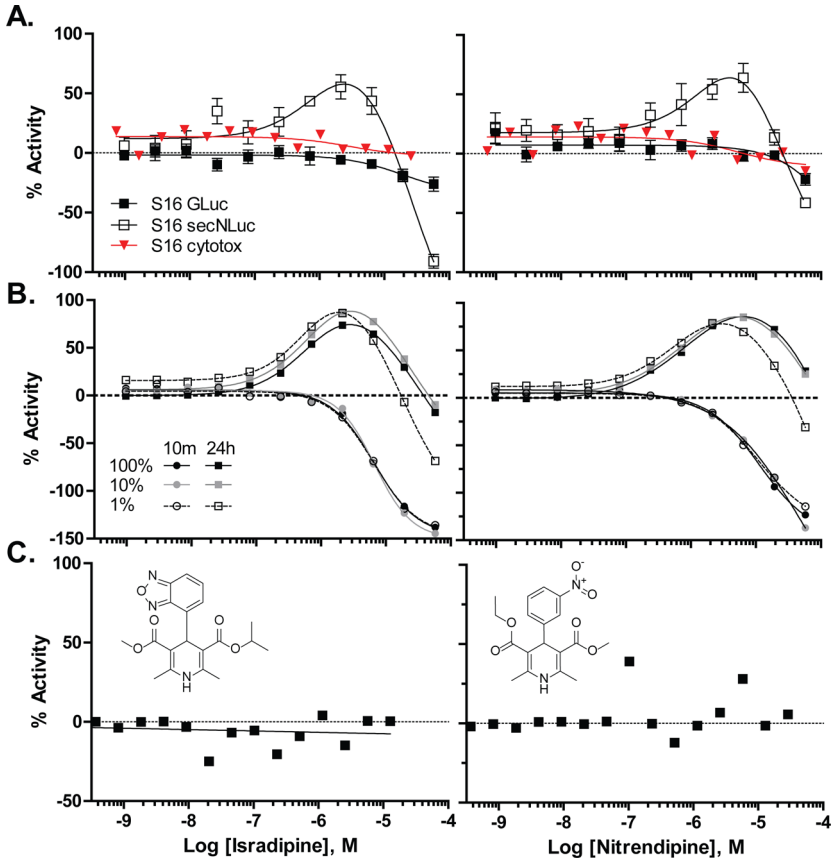

Figure 4. Characterization of reporter-specific inhibitors. (A) CRCs comparing qHTS results from the S16 GLuc (solid square), S16 secNLuc (open square), and cytotoxicity (red triangle) assays for isradipine and nitrendipine activity. (B) Isradipine and nitrendipine activity on NLuc activity as determined from S16 secNLuc cell growth media for varying percentages of media (black, gray, and white symbols) after preincubation for either 10 min (circles) or 24 h (squares). (C) Isradipine and nitrendipine activity on GLuc activity as determined from GLuc-containing cell growth media. Dihydropyridines (DHPs) calcium channel antagonists identified by the secNLuc S16 assay and CRCs of additional DHPs on the enzymatic activity of NLuc enzyme under different concentration of NLuc and incubation times shown in Supplementary Figure 5.

dx.doi.org/10.1021/cb5005492 | ACS Chem. Biol. 2014, 9, 2594–2602

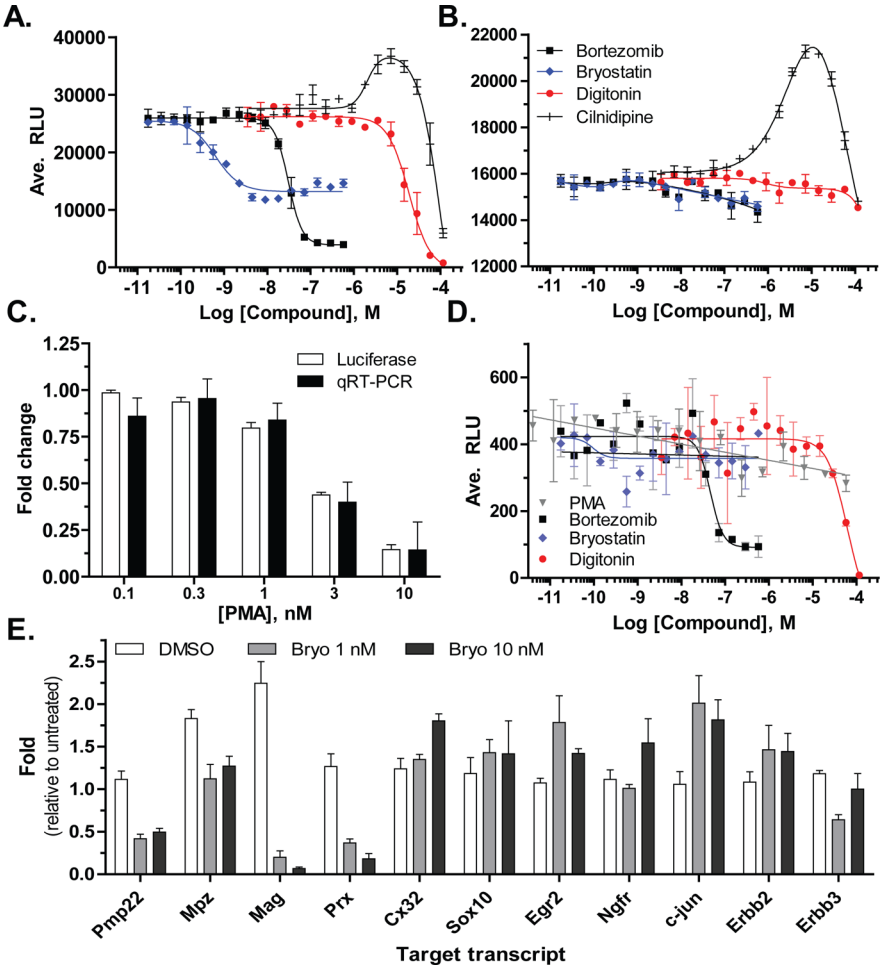

Figure 5. Characterization of PKC modulators. (A) Activity of modulators of *Pmp22* transcription by bryostatin and bortezomib, the NLuc DHP ligand, cilnidipine, and the cytotoxic agent digitonin in the S16 NLuc assay. (B) NLuc enzyme obtained from S16 secNLuc cell culture media and incubated with the compounds in panel A for 24 h prior to determination of NLuc enzyme activity. (C) Phorbol ester, PMA activity on reporter and Pmp22 transcript levels. The secNLuc S16 cell line was plated and exposed to the indicated concentrations of the PMA. At 24 h, NLuc activity was measured from the medium, and RNA was purified from the cells to perform quantitative RT-PCR analysis of Pmp22. Activities and mRNA levels are shown relative to vehicle-treated cells, which were set at 1. (D) Comparative analysis of the compounds in panel A and PMA in the S16 intronic enhancer FLuc assay. Error bars indicate standard deviation of two replicates. (E) Expression analysis of *Pmp22* and co-regulated mRNA transcripts with byrostatin treatment. S16 cells were treated with byrostatin at 1 nM (gray bar) or 10 nM (black bar) or DMSO (0.6%) only (white bar) for 24 h and then applied to qRT-PCR targeting major myelin genes and their regulators. Data were first normalized to ActB and then plotted relative to the untreated sample set to 1 for each target gene. Error bars indicate the SD of three replicates.

From the analysis of the CRCs, potency, efficacy, and preliminary SAR data are used to assess activity of each compound.[34] qHTS also allows a greater degree of discrimination between pharmacological behaviors, as CRC contour can be compared between compounds to assign a sigmoidal versus bell-shaped response (Figure 3A).

Cell-based assays measuring compound-mediated signal inhibition require a strategy to eliminate actives attributable to compound-associated cell toxicity.[35] To this end, we performed a cell toxicity assay as a parallel counter-screen. Drugs with EC_{50}'s for cellular toxicity within 10-fold of the reporter gene assay EC_{50} with nonoverlapping activity in both S16 reporter assays were deprioritized, leaving 31 compounds for further consideration (Supplementary Figure 2). From these compounds we selected representative target class actives to retest. In addition, we included agents with chemotype or MOA similarity, compounds with opposite but detectable responses (e.g., expanded selection of steroids), as well as compounds with non-concordant concentration response relationships between the assays (e.g., the dihydropyridines Ca^{2+} channel antagonists) to investigate the basis of reporter bias in these assays. We compared these 121 compounds (titrated into one 1536-well plate) in both the S16 GLuc and S16 secNLuc assays (Figure 3A; Supplementary Figure 3) to determine an EC_{50} correlation and discern pharmacologic differences from the output.

Our results identify proteasome inhibitors as having similar high potencies and efficacies as originally observed in our enhancer-based FLuc assay[21] (Figure 3B). The assays also detect the very potent effect of several classes of steroids to increase the activity of GLuc and secNLuc (Figure 3C and Supplementary Figure 3). For this latter steroid-associated activity, however, it seems likely that assay noise is attributable to the narrow dynamic range between the inherently high basal signal and the maximal transcriptional activity possible in this cell line, thus affecting automated calling of active compounds in some cases (see Supplementary Figure 4). The progesterone receptor has been identified as a positive regulator of

dx.doi.org/10.1021/cb5005492 | *ACS Chem. Biol.* 2014, 9, 2594−2602

myelination,[36] and a progesterone antagonist, onapristone, has been successfully used in a rat model of CMT1A.[15] While our results support the pharmacological basis of progesterone receptor through the potent action of the synthetic progesterone agonist flugestone on increasing reporter activity, the progesterone antagonist mifepristone displayed marginal effect at inhibiting the basal activity of the reporters (Supplementary Figure 4D). Additionally, the glucocorticoid receptor has been shown to similarly activate *Pmp22* expression,[37] again consistent with our qHTS results (Supplementary Figure 3 and 4).

The design of orthogonal reporter assays aids prioritization of compounds with activities relevant to the biology under investigation, for instance, by controlling for the action of compounds directly on the catalytic activity of the reporter. As an example of reporter bias, we observed reporter-dependent actives among a class of dihydropyridine calcium channel antagonists that display a selective bell-shaped concentration−response profile in the S16 secNLuc assay (Figure 4A). Further evaluation of several dihydropyridines using NLuc enzyme revealed an interesting time-dependent finding illustrated in Figure 4B for representative dihydropyridines isradipine and nitrendipine. Incubation of these or other dihydropyridines (see Supplementary Figure S6) with S16 secNLuc-containing cell culture medium resulted in a clear concentration-dependent inhibition (IC_{50} = 6 μM) of NLuc activity when preincubated with enzyme for 10 min and examined over a 100-fold NLuc concentration range. However, if the dihydropyridines are preincubated with the culture medium-derived NLuc for 24 h prior to measurement of enzyme activity, mimicking the qHTS assay conditions, an apparent increase in enzyme activity was observed as a bell-shaped response (maximum response ∼1.5−2-fold at 3 μM). We reason this to be the result of ligand-induced NLuc stabilization from unfolding or protection from culture medium proteases, related to similar effects we have observed for FLuc stabilization.[35] Despite the similar substrate preference of GLuc and NLuc, dihydropyridines are selective inhibitors of NLuc (Figure 4C). This inhibitor selectivity is most easily explained by the absence of sequence homology between these two proteins, supporting their use as complementary or orthogonal reporters.

Identification of Bryostatin as a Modulator of Pmp22 Expression. One of the most potent modulators of *Pmp22* expression was bryostatin (Figure 5A,B). This compound is a macrolide lactone obtained from a marine invertebrate, *Bugula neritina*. Several different bryostatin-like molecules have been isolated, and all are potent modulators of PKC.[38] Effects on PKC include a short-term activation followed by long-term depression of PKC activity. We initially attempted to modulate *Pmp22* expression using a series of PKC siRNAs (not shown) but did not observe an effect. We used another PKC activator, the phorbol ester PMA, and our results show repression of *Pmp22* reporter expression at nanomolar levels of PMA after 24 h (Figure 5C). Analysis of endogenous *Pmp22* expression levels by quantitative RT-PCR revealed a similar decrease in expression (Figure 5C). The lack of effect using siRNA knockdown of individual PKC subtypes is in line with the lack of potency for several bisindolylmaleimide pan-PKC inhibitors, enzastaurin and Go 6983 (data not shown) and suggests transient activation of PKC is required for the observed effect on *Pmp22* expression.

An important outcome of the present locus-specific integrated reporter study is highlighted by bryostatin, which the previous, randomly integrated reporter assay[21] failed to identify as an inhibitor of *Pmp22*. After completion of the present study, we retested bryostatin on the intronic FLuc assay [23] and again observed no inhibitory effect (Figure 5D). This suggests that locus-specific integrated reporters, the expression of which are presumably modulated by many known and yet unknown factors, are likely to be sensitive to agents that would elude detection based on the activity of a single enhancer. Because of the complexity of transcriptional modulation, this result indicates that reporter insertion in an endogenous gene is more likely to capture molecules that modulate the target in HTS.

To determine the specificity of bryostatin action, we profiled its effect on expression of major transcriptional regulators of Schwann cell differentiation (*Sox10*, *Egr2*, *c-jun*) and major myelin genes that are co-regulated with *Pmp22* during Schwann cell differentiation (*Myelin Protein Zero*, *Myelin-associated glycoprotein*, *Periaxin*, and *Connexin 32/Gjb1*, Figure 5E). The Nerve Growth Factor receptor (p75) is a marker of non-myelinating Schwann cells, while Erbb2/Erbb3 receptors constitute the Schwann cell receptor for axonally derived neuregulin, which is a major signaling pathway regulating Schwann cell differentiation.[39] Consistent with the reporter data, bryostatin lowers *Pmp22* expression to ≤50% of the levels found in untreated S16 cells. In contrast, most of the other tested genes were not affected by bryostatin, with the exception of *Myelin-associated glycoprotein* and *Periaxin*, both of which decline to a greater degree than *Pmp22*.

Conclusion. We used genome editing techniques to embed bioluminescent reporters into the endogenous myelin gene locus in order to perform microtiter 1536-well qHTS screening. By assessing the abundance of secreted reporters, we measure *Pmp22* transcriptional activity and enable a reliable loss-of-signal output configuration assay in a 4 μL volume. Targeted reporter integration at the endogenous locus confirms that pharmacological interrogation of a broader spectrum of mechanisms impacting transcriptional inhibition of *Pmp22* is possible compared to the randomly integrated reporter gene assays used in the previous CMT1A screen.[21] The key important differential finding is our discovery of the potent PKC agonist bryostatin, which had escaped detection in our original random insertion-based assay design.[21] We confirm here that the activity of bryostain is indeed dependent on the contextual features introduced in this new assay design. The identification of bryostatin was further aided by our use of qHTS, as the partial efficacy (Figure 5A) of bryostatin relative to the control, bortezomib, was clearly revealed only by its full titration response profile. The known pharmacology associated with bryostatin[38] allowed us to infer a PKC-associated pathway in the regulation of *Pmp22* transcription, which we confirmed by recapitulation with independent PKC potentiators, PMA and the indole alkaloid (−)-indolactam-V (Figure 5C and Supplementary Figure 3).[40] While the role of PKC in Schwann cell differentiation has not been directly investigated in loss-of-function models, it is likely to regulate MEK-Erk signaling, which can modulate diverse aspects of Schwann cell function.[41]

By using a 3′-directed allele-specific reporter insertion, we maintained the ability to measure the *Pmp22* transcript from the reporter cell line to confirm the fidelity of reporter linkage to *Pmp22* transcription in the subsequent analysis of compounds of interest. A STAT reporter line using ZFNs

dx.doi.org/10.1021/cb5005492 | *ACS Chem. Biol.* 2014, 9, 2594−2602

was recently reported,[42] and HTS has been described using a line derived from homologous recombination;[43] however to our knowledge this is the first application of genome editing technology coupled with high-throughput screening. While the generation of an edited reporter line takes time to construct, these results suggest that such lines could have significant advantages over traditional reporter gene strategies and should be considered as part of future assay designs beyond *Pmp22* and CMT1A.

METHODS

Generation and Maintenance of the S16 Cell Line Expressing *Gaussia* Luciferase. TALE arrays listed in Supplementary Methods were cloned into a TALEN expression vector bearing TALE domain truncation points that enable genome editing activity at endogenous loci.[27] Recombination cassettes for the GLuc reporter and secNLuc reproter clones, and isolation of cell lines were achieved as described in the Supplementary Methods.

Cell-Based *Gaussia* Luciferase (GLuc) and Nanoluciferase (NLuc) Assays. Assays performed in white solid-bottom 1536-well plates used the protocols described in Supplementary Methods and outlined in Supplementary Table 1. Small scale experiments (not using 1536-well plates) employed a previously described protocol for measuring GLuc activity,[44] using either a Promega GloMax plate reader or a single tube Monolight 3010 luminometer. NLuc-expressing S16 cells were plated and treated similar to the GLuc cells, and assays for measuring nanoluciferase activity were purchased from Promega (Madison, WI).

Biochemical GLuc and NLuc Assays. Medium containing either GLuc or NLuc was collected from the culture flasks of either GLuc-expressing or NLuc-expressing S16 cells and assayed as described in the Supplementary Methods.

CellTiter-Glo Assay. The GLuc-expressing and NLuc-expressing S16 cells were dispensed into white solid-bottom 1536-well plates, incubated with compounds for 24 h at 37 °C, after which 1 volume of CellTiter-Glo luminescent cell viability assay reagent (Promega) was added using a BioRAPTR FRD. Luminescence was measured as described above; additional information is in Supplementary Methods.

Quantitative Reverse Transcription-PCR Analysis. qRT-PCR was carried out essentially as previously described.[21] In 6-well plates cells (2×10^5 cells/well) were plated and treated with either DMSO or bryostatin. After 24 h, the cells were harvested using an RNeasy Plus Micro kit (Qiagen) for purification of RNA, which was converted into cDNA using superscript III first-strand synthesis supermix (Invitrogen). Quantitative PCR was performed in either SYBR green-based reactions or Taqman-based customized 384-well micro fluidic arrays using a ViiA7 system (Applied biosystems, Foster City, CA). See Supplementary Methods for details and Supplementary Table 3 for primer sequences.

Western Blot Analysis. S16 cells were plated in 6-well tissue culture plates and treated with each siRNA as described.[21] After 24 h, lysates were harvested and analyzed by immunoblotting for PMP22 (1:1000, cat. no. ab61220, Abcam) as described.[21]

Data Analysis for qHTS. Data from each assay was normalized plate-wise to corresponding intraplate controls as described previously[34] and elaborated on in the Supplementary Methods. To discern if the response of the assay system for each re-acquired compound was best fit by a 3- or 4-parameter (Hill equation) or 5-parameter (bell-shaped curve) model, the aggregated data sets for each of 4 or 8 runs of the compounds for each assay type were fit using GraphPad Prism. The equation with the lower number of parameters was used as the null hypotheses, and the equation with more parameters used as the alternate hypotheses and fits compared using the extra sum-of-squares F test. Additional details are given in the Supplementary Methods.

ASSOCIATED CONTENT

Supporting Information

Full methods and supplemental data. This material is available free of charge via the Internet at http://pubs.acs.org.

AUTHOR INFORMATION

Corresponding Authors

*E-mail: jinglese@mail.nih.gov.
*E-mail: jpsvaren@wisc.edu.

Notes

The authors declare no competing financial interest.

ACKNOWLEDGMENTS

From NCATS we thank P. Shinn and S. Michael for management of compound libraries and robotic screening support, respectively, and M. Mendez and B. Wright for constructive comments to the manuscript; from UW, E. Lau for assistance in cell culture, and the UWCCC Flow Laboratory for assistance flow sorting; and from Sangamo BioSciences the Technology and Production groups for nuclease design and assembly and E. Rebar, F. Urnov, and P. Gregory for comments to the manuscript. This work was supported by the intramural program of NCATS and the Charcot–Marie–Tooth Association (J.I.), grants from the National Institutes of Health/NINDS (R21 NS73726) (J.S.), and P30 core grant HD03352.

REFERENCES

(1) Reilly, M. M., Murphy, S. M., and Laurá, M. (2011) Charcot–Marie–Tooth disease. *J. Peripher. Nerv. Syst. 16*, 1–14.
(2) Shy, M. E., Chen, L., Swan, E. R., Taube, R., Krajewski, K. M., Herrmann, D., Lewis, R. A., and McDermott, M. P. (2008) Neuropathy progression in Charcot–Marie–Tooth disease type 1A. *Neurology 70*, 378–383.
(3) Patzkó, A., and Shy, M. E. (2011) Update on Charcot–Marie–Tooth disease. *Curr. Neurol. Neurosci. Rep. 11*, 78–88.
(4) Saporta, A. S., Sottile, S. L., Miller, L. J., Feely, S. M., Siskind, C. E., and Shy, M. E. (2011) Charcot–Marie–Tooth disease subtypes and genetic testing strategies. *Ann. Neurol. 69*, 22–33.
(5) Murphy, S. M., Laura, M., Fawcett, K., Pandraud, A., Liu, Y. T., Davidson, G. L., Rossor, A. M., Polke, J. M., Castleman, V., Manji, H., Lunn, M. P., Bull, K., Ramdharry, G., Davis, M., Blake, J. C., Houlden, H., and Reilly, M. M. (2012) Charcot–Marie–Tooth disease: frequency of genetic subtypes and guidelines for genetic testing. *J. Neurol., Neurosurg. Psychiatry 83*, 706–710.
(6) Patel, P. I., Roa, B. B., Welcher, A. A., Schoener-Scott, R., Trask, B. J., Pentao, L., Snipes, G. J., Garcia, C. A., Francke, U., Shooter, E. M., Lupski, J. R., and Suter, U. (1992) The gene for the peripheral myelin protein PMP-22 is a candidate for Charcot–Marie–Tooth disease type 1A. *Nat. Genet. 1*, 159–165.
(7) Timmerman, V., Nelis, E., Van Hul, W., Nieuwenhuijsen, B. W., Chen, K. L., Wang, S., Ben Othman, K., Cullen, B., Leach, R. J., and Hanemann, C. O. (1992) The peripheral myelin protein gene PMP-22 is contained within the Charcot–Marie–Tooth disease type 1A duplication. *Nat. Genet. 1*, 171–175.
(8) Huxley, C., Passage, E., Manson, A., Putzu, G., Figarella-Branger, D., Pellissier, J. F., and Fontes, M. (1996) Construction of a mouse model of Charcot–Marie–Tooth disease type 1A by pronuclear injection of human YAC DNA. *Hum. Mol. Genet. 5*, 563–569.
(9) Huxley, C., Passage, E., Robertson, A. M., Youl, B., Huston, S., Manson, A., Saberan-Djoniedi, D., Figarella-Branger, D., Pellissier, J. F., Thomas, P. K., and Fontes, M. (1998) Correlation between varying levels of PMP22 expression and the degree of demyelination and reduction in nerve conduction velocity in transgenic mice. *Hum. Mol. Genet. 7*, 449–458.
(10) Magyar, J. P., Martini, R., Ruelicke, T., Aguzzi, A., Adlkofer, K., Dembic, Z., Zielasek, J., Toyka, K. V., and Suter, U. (1996) Impaired

differentiation of Schwann cells in transgenic mice with increased PMP22 gene dosage. *J. Neurosci. 16*, 5351−5360.
(11) Robertson, A. M., Perea, J., McGuigan, A., King, R. H., Muddle, J. R., Gabreels-Festen, A. A., Thomas, P. K., and Huxley, C. (2002) Comparison of a new pmp22 transgenic mouse line with other mouse models and human patients with CMT1A. *J. Anat. 200*, 377−390.
(12) Sereda, M., Griffiths, I., Puhlhofer, A., Stewart, H., Rossner, M. J., Zimmerman, F., Magyar, J. P., Schneider, A., Hund, E., Meinck, H. M., Suter, U., and Nave, K. A. (1996) A transgenic rat model of Charcot−Marie−Tooth disease. *Neuron 16*, 1049−1060.
(13) Passage, E., Norreel, J. C., Noack-Fraissignes, P., Sanguedolce, V., Pizant, J., Thirion, X., Robaglia-Schlupp, A., Pellissier, J. F., and Fontes, M. (2004) Ascorbic acid treatment corrects the phenotype of a mouse model of Charcot−Marie−Tooth disease. *Nat. Med. 10*, 396−401.
(14) Perea, J., Robertson, A., Tolmachova, T., Muddle, J., King, R. H., Ponsford, S., Thomas, P. K., and Huxley, C. (2001) Induced myelination and demyelination in a conditional mouse model of Charcot−Marie−Tooth disease type 1A. *Hum. Mol. Genet. 10*, 1007−1018.
(15) Sereda, M. W., Meyer zu Horste, G., Suter, U., Uzma, N., and Nave, K. A. (2003) Therapeutic administration of progesterone antagonist in a model of Charcot−Marie−Tooth disease (CMT-1A). *Nat. Med. 9*, 1533−1537.
(16) Lewis, R. A., McDermott, M. P., Herrmann, D. N., Hoke, A., Clawson, L. L., Siskind, C., Feely, S. M., Miller, L. J., Barohn, R. J., Smith, P., Luebbe, E., Wu, X., Shy, M. E., and Group, M. S. (2013) High-dosage ascorbic acid treatment in Charcot−Marie−Tooth disease type 1A: results of a randomized, double-masked, controlled trial. *JAMA Neurol. 70*, 981−987.
(17) Topilko, P., Schneider-Maunoury, S., Levi, G., Baron-Van Evercooren, A., Chennoufi, A. B., Seitanidou, T., Babinet, C., and Charnay, P. (1994) Krox-20 controls myelination in the peripheral nervous system. *Nature 371*, 796−799.
(18) Britsch, S., Goerich, D. E., Riethmacher, D., Peirano, R. I., Rossner, M., Nave, K. A., Birchmeier, C., and Wegner, M. (2001) The transcription factor Sox10 is a key regulator of peripheral glial development. *Genes Dev. 15*, 66−78.
(19) Jones, E. A., Lopez-Anido, C., Srinivasan, R., Krueger, C., Chang, L. W., Nagarajan, R., and Svaren, J. (2011) Regulation of the PMP22 gene through an intronic enhancer. *J. Neurosci. 31*, 4242−4250.
(20) Huang, R., Southall, N., Wang, Y., Yasgar, A., Shinn, P., Jadhav, A., Nguyen, D. T., and Austin, C. P. (2011) The NCGC pharmaceutical collection: a comprehensive resource of clinically approved drugs enabling repurposing and chemical genomics. *Sci. Transl. Med. 3*, 80ps16.
(21) Jang, S. W., Lopez-Anido, C., MacArthur, R., Svaren, J., and Inglese, J. (2012) Identification of drug modulators targeting gene-dosage disease CMT1A. *ACS Chem. Biol. 7*, 1205−1213.
(22) Verrier, J. D., Lau, P., Hudson, L., Murashov, A. K., Renne, R., and Notterpek, L. (2009) Peripheral myelin protein 22 is regulated post-transcriptionally by miRNA-29a. *Glia 57*, 1265−1279.
(23) Lau, P., Verrier, J. D., Nielsen, J. A., Johnson, K. R., Notterpek, L., and Hudson, L. D. (2008) Identification of dynamically regulated microRNA and mRNA networks in developing oligodendrocytes. *J. Neurosci. 28*, 11720−11730.
(24) Jones, E. A., Brewer, M. H., Srinivasan, R., Krueger, C., Sun, G., Charney, K. N., Keles, S., Antonellis, A., and Svaren, J. (2012) Distal enhancers upstream of the Charcot−Marie−Tooth type 1A disease gene PMP22. *Hum. Mol. Genet. 21*, 1581−1591.
(25) Weterman, M. A., van Ruissen, F., de Wissel, M., Bordewijk, L., Samijn, J. P., van der Pol, W. L., Meggouh, F., and Baas, F. (2010) Copy number variation upstream of PMP22 in Charcot−Marie−Tooth disease. *Eur. J. Hum. Genet. 18*, 421−428.
(26) Zhang, F., Seeman, P., Liu, P., Weterman, M. A., Gonzaga-Jauregui, C., Towne, C. F., Batish, S. D., De Vriendt, E., De Jonghe, P., Rautenstrauss, B., Krause, K. H., Khajavi, M., Posadka, J., Vandenberghe, A., Palau, F., Van Maldergem, L., Baas, F., Timmerman, V., and Lupski, J. R. (2010) Mechanisms for non-recurrent genomic rearrangements associated with CMT1A or HNPP: rare CNVs as a cause for missing heritability. *Am. J. Hum. Genet. 86*, 892−903.
(27) Miller, J. C., Tan, S., Qiao, G., Barlow, K. A., Wang, J., Xia, D. F., Meng, X., Paschon, D. E., Leung, E., Hinkley, S. J., Dulay, G. P., Hua, K. L., Ankoudinova, I., Cost, G. J., Urnov, F. D., Zhang, H. S., Holmes, M. C., Zhang, L., Gregory, P. D., and Rebar, E. J. (2011) A TALE nuclease architecture for efficient genome editing. *Nat. Biotechnol. 29*, 143−148.
(28) Carroll, D. (2014) Genome engineering with targetable nucleases. *Annu. Rev. Biochem. 83*, 409−439.
(29) Toda, K., Small, J. A., Goda, S., and Quarles, R. H. (1994) Biochemical and cellular properties of three immortalized Schwann cell lines expressing different levels of the myelin-associated glycoprotein. *J. Neurochem. 63*, 1646−1657.
(30) Fang, J., Qian, J. J., Yi, S., Harding, T. C., Tu, G. H., VanRoey, M., and Jooss, K. (2005) Stable antibody expression at therapeutic levels using the 2A peptide. *Nat. Biotechnol. 23*, 584−590.
(31) Tannous, B. A., Kim, D. E., Fernandez, J. L., Weissleder, R., and Breakefield, X. O. (2005) Codon-optimized Gaussia luciferase cDNA for mammalian gene expression in culture and in vivo. *Mol. Ther. 11*, 435−443.
(32) Hall, M. P., Unch, J., Binkowski, B. F., Valley, M. P., Butler, B. L., Wood, M. G., Otto, P., Zimmerman, K., Vidugiris, G., Machleidt, T., Robers, M. B., Benink, H. A., Eggers, C. T., Slater, M. R., Meisenheimer, P. L., Klaubert, D. H., Fan, F., Encell, L. P., and Wood, K. V. (2012) Engineered luciferase reporter from a deep sea shrimp utilizing a novel imidazopyrazinone substrate. *ACS Chem. Biol. 7*, 1848−1857.
(33) Ho, P. I., Yue, K., Pandey, P., Breault, L., Harbinski, F., McBride, A. J., Webb, B., Narahari, J., Karassina, N., Wood, K. V., Hill, A., and Auld, D. S. (2013) Reporter enzyme inhibitor study to aid assembly of orthogonal reporter gene assays. *ACS Chem. Biol. 8*, 1009−1017.
(34) Inglese, J., Auld, D. S., Jadhav, A., Johnson, R. L., Simeonov, A., Yasgar, A., Zheng, W., and Austin, C. P. (2006) Quantitative high-throughput screening: a titration-based approach that efficiently identifies biological activities in large chemical libraries. *Proc. Natl. Acad. Sci. U.S.A. 103*, 11473−11478.
(35) Thorne, N., Inglese, J., and Auld, D. S. (2010) Illuminating insights into firefly luciferase and other bioluminescent reporters used in chemical biology. *Chem. Biol. 17*, 646−657.
(36) Chan, J. R., Phillips, L. J., and Glaser, M. (1998) Glucocorticoids and progestins signal the initiation and enhance the rate of myelin formation. *Proc. Natl. Acad. Sci. U.S.A. 95*, 10459−10464.
(37) Désarnaud, F., Bidichandani, S., Patel, P. I., Baulieu, E. E., and Schumacher, M. (2000) Glucocorticosteroids stimulate the activity of the promoters of peripheral myelin protein-22 and protein zero genes in Schwann cells. *Brain Res. 865*, 12−16.
(38) Ruan, B. F., and Zhu, H. L. (2012) The chemistry and biology of the bryostatins: potential PKC inhibitors in clinical development. *Curr. Med. Chem. 19*, 2652−2664.
(39) Taveggia, C., Feltri, M. L., and Wrabetz, L. (2010) Signals to promote myelin formation and repair. *Nat. Rev. Neurol. 6*, 276−287.
(40) Wu-Zhang, A. X., and Newton, A. C. (2013) Protein kinase C pharmacology: refining the toolbox. *Biochem. J. 452*, 195−209.
(41) Pereira, J. A., Lebrun-Julien, F., and Suter, U. (2012) Molecular mechanisms regulating myelination in the peripheral nervous system. *Trends Neurosci. 35*, 123−134.
(42) Samsonov, A., Zenser, N., Zhang, F., Zhang, H., Fetter, J., and Malkov, D. (2013) Tagging of genomic STAT3 and STAT1 with fluorescent proteins and insertion of a luciferase reporter in the cyclin D1 gene provides a modified A549 cell line to screen for selective STAT3 inhibitors. *PLoS One 8*, e68391.
(43) Lyssiotis, C. A., Foreman, R. K., Staerk, J., Garcia, M., Mathur, D., Markoulaki, S., Hanna, J., Lairson, L. L., Charette, B. D., Bouchez, L. C., Bollong, M., Kunick, C., Brinker, A., Cho, C. Y., Schultz, P. G., and Jaenisch, R. (2009) Reprogramming of murine fibroblasts to

induced pluripotent stem cells with chemical complementation of Klf4. *Proc. Natl. Acad. Sci. U.S.A. 106*, 8912−8917.
(44) Tannous, B. A. (2009) Gaussia luciferase reporter assay for monitoring biological processes in culture and in vivo. *Nat. Protoc. 4*, 582−591.